The effect of the pH value on microporous TiO_2/ZnO heterostructure

Tao Zeng
College of International Education
Mudanjiang Normal University
Mudanjiang
157011, China

Abstract—A novel microporous ZnO/TiO_2 heterostructure, which consists of crystalline TiO_2 decorated with amorphous ZnO, have been fabricated by a facile one-step synthetic methods. The results showed that the phase composition of the growing units and the intrinsic crystal structure are seriously controlled by the synthetic environment. Particularly, we have successfully captured the transformation process of the amorphous/crystalline heterostructure by adjusting the pH value. A microporous TiO2/ZnO composite photocatalyst consisting of crystalline TiO_2 nanoparticles decorated with amorphous ZnO is fabricated by low-temperature hydrothermal treatment. And the pH value during the preparation of the new configuration photocatalyst affects the crystalline structure and BET surface area. The sample with high pH value (8~12) is favorable to the formation of an amorphous/crystalline composite structure with large micropore area and BET surface area. When the pH value is 12, the novel photocatalyst not only exhibits the excellent photocatalytic activity of hydrogen evolution from water splitting, but also has a large micropore area.

Keywords-TiO_2/ZnO composites; Photocatalytic; PH value; Hydrothermal treatment; Heterostructure;

I. INTRODUCTION

During the past decades, TiO_2-based semiconductor materials have been widely used in environmental pollution control and solar-driven hydrogen production for the low cost, non-toxicity, and high chemical stability [1-3]. However, due to the high recombination of photogenerated electrons and holes in excited TiO_2, TiO_2 suffers from low efficiency or instability for hydrogen evolution from water splitting under the irradiation of solar light. Recently, ions doping, surface modification and exploring different hybrid semiconductor heterostructure have been used to improve the performance of TiO_2 [4-8]. TiO_2/ZnO heterostructures have been extensively studied for light absorption, light-electron conversion and electron transportation processes [9-11]. Since TiO_2 and ZnO have different band gaps, when excited electrons in TiO_2 with a lower conduction band minimum (CBM) recombine with the holes in ZnO with a higher valence band maximum (VBM), more powerful excited electrons and holes can be retained on different counterparts, which possesses a favorable photocatalytic water splitting capability. Up to date, various preparation methods have been explored for the synthesis of TiO_2/ZnO heterostructures. However, there is no discussion about the phase control of them, which plays an important role on improving the photocatalytic activity.

Besides the above issues, porosity, specific surface area and crystal form are also crucial for a high performance photocatalyst. Large specific surface area and porous can provide sufficient interface for the photocatalytic reaction, while crystal form is more important for the photocatalytic activity of photocatalyst [12-18]. Amorphous, in contrast to its crystalline part, the unordered structure could capture electrons easily, and thus forcibly separate the pairs of electrons/holes on the crystal and reduce their recombination effectively, facilitating the photocatalytic activity of the catalyst. It has been reported that amorphous materials have special performance in the field of heterogeneous catalysis and other areas for their novel structures and electronic characters.

In this study, structure-controlled TiO_2/ZnO heterostructure has been synthesized by a simple and effective route. And different phase composition of TiO_2/ZnO heterostructure can be obtained by adjusting the experimental parameters. The result finds that the pH value during the preparation plays an important role on the phase composition the samples.

II. EXPERIMENTAL

A. Catalyst preparation

All chemicals were used as received, without further purification. The detailed experimental description can refer to previous paper. The pH value of the solution is adjusted to 4, 6, 8, 10 and 12 by sodium hydroxide solution. Then solution C was transferred to a 100mL teflon-lined stainless steel autoclave after being stirred for 2 h, followed by a hydrothermal treatment at 120 ℃ for 12 h. The corresponding product was denoted as TZ4, TZ6 and TZ8.

B. Characterization techniques

X-ray diffraction (XRD) patterns were collected on a Rigaku D/max-2200VPC diffractometer. N2 adsorption-desorption isotherms were recorded on a Micromeritics ASAP 2020 surface area and porosity analyzer. The specific surface area was obtained by the Brunauer-Emmett-Teller (BET) method, and pore size distribution was calculated from the adsorption branch of the isotherm by density functional theory (DFT) method.

III. RESULTS AND DISCUSSION

A. XRD analysis

Fig .1 shows XRD patterns of TZ4, TZ6 and TZ8. It can be found that all the samples show simple anatase

phase, without the existence of ZnO or other impurities. Thus pH value plays a crucial role in determining the phase composition of TiO_2/ZnO heterostructure. For TZ4 and TZ6, there are no characteristic peaks belonging to amorphous can be found. While for TZ8, amorphous/crystalline composite phase can be observed.

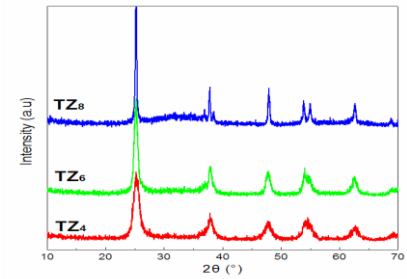

Figure 1. XRD spectra of the prepared prepared samples with different pH value.

B. SEM analysis

Fig .2 showed the SEM images of TZ4, TZ6 and TZ8. Clearly, the average crystallite size of the samples increased with increasing of the pH values. Moreover, the dispersibility of the particles gets obviously improvement when the pH value is high. The influence of pH value on the phase and morphology can be ascribed to the concentration of hydroxyl groups that mainly changes the ionic super saturation.

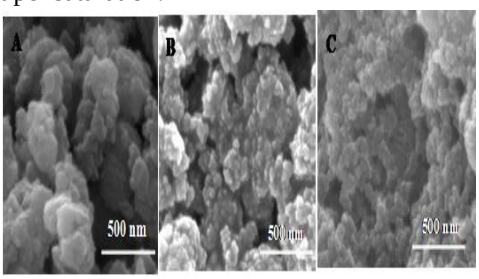

Figure 2. SEM images of the prepared prepared samples with different pH value.

C. Surface area analysis

Fig .3 displays the N_2 adsorption–desorption isotherms of the samples with various pH value. Obviously, when the pH value is 4 and 6, the isotherms of them exhibit Type IV isotherms, indicating the presence of well-developed mesopores in the samples. When the pH is up to 8, and the specific surface areas of them are 182 $m^2 \cdot g^{-1}$.The micropore area and pore size are summarized in Table I

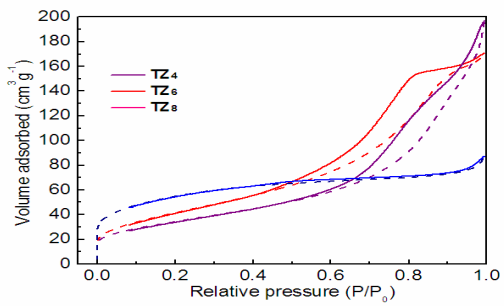

Figure 3. N_2 adsorption-desorption isotherms of the samples with various pH values

TABLE I Summary of the physicochemical properties of the TZ3 samples.

pH in solution	micropore area[b] ($m^2 \cdot g^{-1}$)	Pore size[c] (nm)	Morphology
4	_	9.8	Anatase
6	_	6.8	Anatase
8	13.6	4.9	Amorphous/ anatase

D. XPS analysis

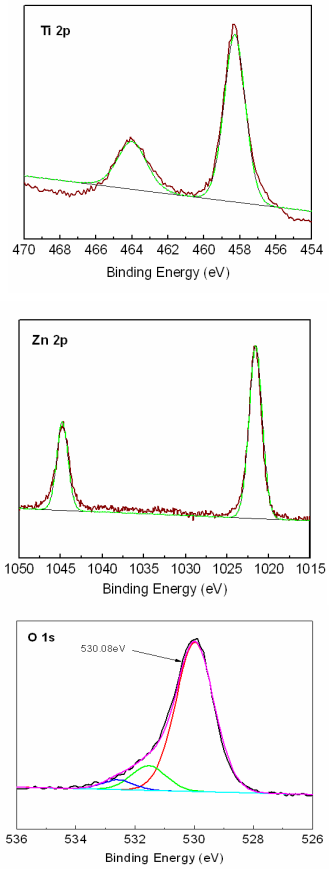

Figure 4. The XPS spectra of TiO_2/ZnO heterostructure with Zn/Ti ration of 1/3, Ti 2p, Zn 2p and O 1s

The bonding states of the TZ3 (amorphous/crystalline composite structure) were characterized by XPS. Fig .4 shows the O1s, Ti 2p and Zn 2p core level XPS spectra of the TZ3. The O 1s of TZ3 showed two peaks, which is located at 529.8 eV and 531.5 eV corresponding to Ti–O and Zn–O bonds, respectively. The binding energy of Ti 2p3/2 is centered at 459.28 eV corresponding to Ti^{4+}, which is consist with Ti-O bond of anatase based on the XRD result. The Zn 2p peak was observed at 1021.4 eV corresponding to Zn-O bond. While there is no crystalline ZnO exist in the above XRD result, thus we implied that ZnO was probably present as amorphous or partly doped in TiO_2.

E. *Photocatalytic activity*

$$h^+ + H_2O \rightarrow \cdot OH + H^+ \quad (a)$$

$$CH_3OH + \cdot OH \rightarrow \cdot CH_2OH + H_2O \quad (b)$$

$$\cdot CH_2OH \rightarrow HCHO + H^+ + e^- \quad (c)$$

$$2H_2O + 2e^- \rightarrow H_2 + 2OH^- \quad (d)$$

We tested the water splitting system in pure water or under the condition of formaldehyde as sacrificial reagent (Fig .5). Here, in order to save the test time, we choose pure TiO_2 (control sample), pure ZnO (control sample), $TZ3_4$ (crystalline structure), $TZ3_8$ ("thin" amorphous/crystalline structure) and $TZ3_{12}$ ("thick" amorphous/crystalline structure) as the representative samples. Fig .5 shows the pure water splitting result with no sacrificial reagent. Obviously, the photocatalyst activities of the samples has fallen compared with the water splitting system in the presence of methanol as sacrificial reagent, especially the pure TiO_2 and pure ZnO showed a worse activity. Certainly, methanol as a well-known sacrificial reagent plays an important role in the water splitting system. When the system is constructed in the presence of sacrificial reagent (electron donor), the photogenerated holes irreversibly oxidize the reducing electron donors instead of H_2O, facilitates water reduction by the photogenerated electrons in the conduction band. The following (a-d) is the reaction steps of methanol.

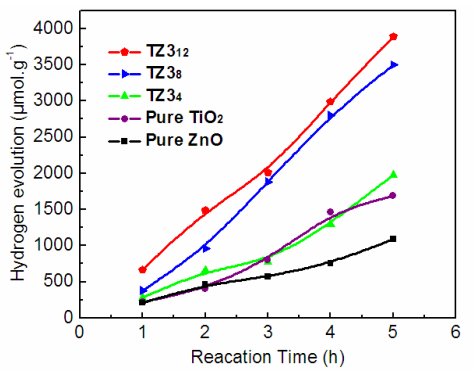

Figure 5. Water splitting system using formaldehyde as sacrificial reagent

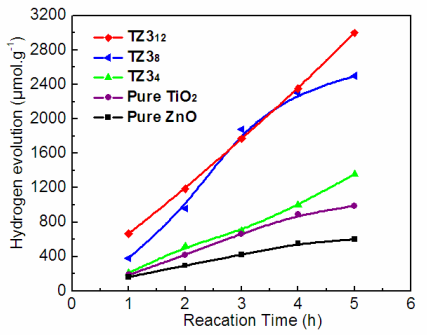

Figure 6. Water splitting system without sacrificial reagent

Water splitting result using formaldehyde as sacrificial reagent is showed in the following Fig .6, it can be found that the $TZ3_{12}$ sample with amorhpus/crystalline composite structure also exhibited an enhanced H_2 producitivity.

The basic principle of photocatalytic reactions for hydrogen/oxygen generation using electron donors/acceptors as the sacrificial reagent is depicted in the following Schema (Fig .7). In the water splitting process, the e^-/h^+ pairs photogenerated in the TiO_2 particles upon photoexcitation will migrate to their surfaces where these redox reactions take place. As you said, the oxidation of methanol is faster than the oxidation of water, and we appreciate your kind suggestions. On the oxidative side, the photogenerated holes will either react with surface Ti–OH groups producing trapped holes or with adsorbed water molecules producing adsorbed •OH radicals or they will be transferred directly to adsorbed methanol molecules. However, it seems difficult to learn the differentiation between these pathways, and the exact source of the protons yielding H_2 cannot be determined clearly, i.e., it is unclear whether H^+ originates from water or from CH_3OH. Certainly, it seems indicate that methanol acts as the only hole scavenger resulting in H_2 production. Since methanol is a well-known sacrificial reagent, thus there are many papers used methanol as sacrificial reagent.

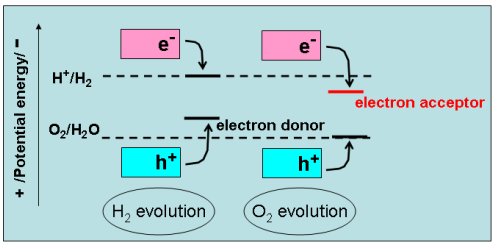

Figure 7. The role of the sacrificial reagent in the the water splitting system

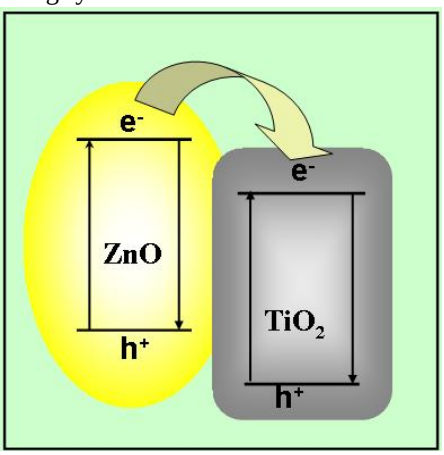

Figure 8. The schema of conduction bands between ZnO and TiO_2

Fig .8 shows the schema of conduction bands between ZnO and TiO_2 The difference in the positions of conduction bands between ZnO and TiO_2 drives photoelectrons in ZnO to surrounding TiO_2 nanoparticles

immediately upon light absorption, thus forcibly separate the pairs of electrons/holes on the surface and reduce their recombination effectively, facilitating the photocatalytic activity of the catalyst. While in contrast to the crystalline TiO_2, the surface modifying amorphous ZnO exhibited intimate contact with the base TiO_2 by forming heterostructure which resulted in much easier charge transfer and better separation efficiency.

IV. CONCLUSIONS

The microporous TiO_2/ZnO with amorphous/crystalline heterostructure composite catalyst has been prepared by a low-temperature hydrothermal synthesis. The result confirms that the pH value not only influences the phase composition, but also has a significant impact on micropore area of the sample. The synergistic effect of the amorphous/crystalline phase structure of TiO_2/ZnO heterostructure composite and the high specific surface area of this low-temperature synthesis process could contribute to the enhancement of the photocatalytic activity.

ACKNOWLEDGEMENTS

The present work is supported by "Youth Scholar Backbone Supporting Plan of General Colleges and Universities" (1253G059).

REFERENCE

[1] X.W. Wang, G. Liu, G.Q. Lu, H.M. Cheng, Int. J. Hydrogen Energy 35 (2010) 8199–8205.

[2] Y. Huo, X. Yang, J. Zhu, H. Li, Appl. Catal. B: Environ. 106 (2011) 69–75.

[3] R. Ciancio, E. Carlino, C. Aruta, D. Maccariello, F.M. Granozio, U.S.D. Uccio, Nanoscale 4 (2012) 91-94.

[4] J.S. Chen, D.Y. Luan, C.M. Li, F.Y.C. Boey, S.Z. Qiao, X.W. Lou, Chem. Commun. 46 (2010) 8252-8254.

[5] I.L. Hsiao, Y.J. Huang, Chem. Res. Toxicol. 24 (2011) 303.

[6] J.S. Jang, H.G. Kim, P.H. Borse, J.S. Lee, Int. J. Hydrogen Energy 32 (2007) 4786-4791.

[7] H. Cao, S.L. Sui, J. Am. Chem. Soc. 116 (1994) 5334-5342.

[8] J.M. Yan, X.B. Zhang, S. Han, H. Shioyama, Q. Xu, Angew. Chem. Int. Ed. 47 (2008) 2287-2289.

[9] L.F. Cui, R. Ruffo, C.K. Chan, H.L. Peng, Y. Cui, Nanoletters 9 (2009) 491-495.

[10] X.B. Zhang, J.M. Yan, S. Han, H. Shioyama, Q. Xu, J. Am. Chem. Soc. 131 (2009) 2778-2779.

[11] Y.J. Chen, P. Gao, R.X. Wang, C.L. Zhu, L.J. Wang, M.S. Cao, H.B. Jin, J. Phys. Chem. C 113 (2009) 10061-10064.

[12] A. A. Ismail, D. W. Bahnemannb, J. Mater. Chem. 21 (2011) 11686-11707.

[13] C. Jin, R.Y. Zheng, Y. Guo, J.L. Xie, Y.X. Zhu, Y.C. Xie, J Mol Catal A-Chem. 313 (2009) 44-48.

[14] P. Kubiak, T. Froeschl, N. Huesing, U. Hoermann, U. Kaiser, R. Schiller, C. K. Weiss, K. Landfester and M. WohlfahrtMehrens, Small 7 (2011) 1690–1696.

[15] L.H. Chang, N. Sasirekha, Y.W. Chen, Catal. Commun. 8 (2007) 1702-1710.

[16] A. Beck, G. Magesh, B. Kuppan, Z. Schay, O. Geszti, T. Benko, R. P. Viswanath, P. Selvam, B. Viswanathan and L. Guczi, Catal. Today 164 (2011) 325–331.

[17] T. Sreethawong, S. Laehsalee and S. Chavadej, Catal. Commun.10 (2009) 538-543.

[18] M.T. Tsai, Y.U. Chang, H.L. Huang, J.T. Hsu, Y.C. Chen, A.Y.J. Wu, Thin Solid Films 528 (2013) 143–150.